Chapter 1

Fundamentals

Seventy years ago, satellite meteorology did not exist except perhaps in science fiction. Today, the latest satellite images of the world's weather and animated sequences of tropical storms are being shown on our television sets and available on our mobiles. The fascinating origin of this new branch of meteorology, and its phenomenal growth, have indeed had a touch of fantasy. What satellite meteorology happens to be today, is the result of an interplay of science on one hand, and the technology of satellites, computers and communications on the other. Limitations of technology have been overcome by scientific ingenuity, and the requirements of science have driven technology to the cutting edge.

After the successful launch of the first weather satellite TIROS-1 in 1960 and the growth of satellite coverage of the earth's atmosphere and oceans within just a decade afterwards, meteorologists were in fact overwhelmed by the new satellite data that became available to them. Prior to the satellite era, meteorologists had laid the greatest emphasis on atmospheric pressure. Lows and highs showing up in synoptic isobaric analysis were of their main interest and many other weather elements including cloud cover, although observed, were not analyzed on a synoptic scale in a similar manner. With the availability of satellite images, however, the accent shifted to observing and examining clouds and cloud patterns in the imagery, from which the state of the atmosphere could be directly observed or inferred. Images received from geostationary and orbiting satellites together revealed the presence of a wide spectrum of atmospheric phenomena across individual cumulus cells, thunderstorms, tropical cyclones and jet streams, just at a glance. So much so, that ground weather observation stations began to face the risk of redundancy and closure. Competition from satellite imagery forced many national meteorological services to take a re-look at their network configurations and trim them, particularly the upper air stations which are expensive to operate and maintain.

Whether satellites can give us all that we need for weather analysis and forecasting has been a subject of debate, what is unquestionable is the fact that satellites have been giving us more and more than we ever anticipated. Satellites are no longer playing just a supportive role in meteorology but they

are becoming independent and intelligent systems that would manage climate change, disaster response and sustainable development.

Whatever be the scenario, present or future, the fundamental principles of satellite meteorology do not change with time and they are discussed in the following sections of this chapter.

1.1 Principles of Meteorological Remote Sensing

Remote sensing has been defined in various ways, but it is basically the process of observing an object without going near it or touching it, and that too in wavelengths that the human eye cannot perceive. Remote sensing of the earth and its atmosphere was a novel idea in the mid-20th century and was done primarily by taking photographs from aircrafts. Soon thereafter it developed into a satellite-based technique for measurement of radiation from the sun and the earth. Remote sensing satellites were launched for monitoring the earth's natural resources and meteorological satellites for observing the atmosphere.

1.1.1 Electromagnetic Spectrum

By the term spectrum, we traditionally mean the seven colours of visible light, such as those seen in a rainbow. Nowadays, the term has come to be associated more with mobile communications along with terms like 4G or 5G. In scientific parlance, however, it refers to the entire range of wavelength or frequency of electromagnetic radiation, visible light or the microwave region being just small parts of it (Table 1.1.1.1). The characteristic spectrum of a given object is the pattern of electromagnetic radiation that it absorbs, transmits and emits.

The product of the wavelength λ and frequency ν of electromagnetic waves is equal to c, the velocity of light. The associated energy $E = h.\nu = h.c / \lambda$ where h is Planck's constant. This means that as the wavelength of electromagnetic radiation increases, its frequency decreases and the associated energy gets reduced.

The region of the electromagnetic spectrum with which we are most concerned in real life is the region of visible light, to which the human eye is very sensitive and in which the sun and stars emit the strongest radiation. In recent times, we are getting familiar with other wavelength regions as FM radio stations, mobile phones, satellite television or microwave ovens become more and more a part of our daily life.

Table 1.1.1.1 Electromagnetic Spectrum.

<table>
<tr><th>Wavelength</th><th></th><th>Wavelength</th><th></th></tr>
<tr><td>10^{-6} nm</td><td rowspan="4">Gamma Rays
(MeV)</td><td>1 mm</td><td>Millimetre
Waves (mm)</td></tr>
<tr><td>10^{-5} nm</td><td>1 cm</td><td rowspan="3">Microwaves
(cm, GHz)</td></tr>
<tr><td>10^{-4} nm</td><td>10 cm</td></tr>
<tr><td>10^{-3} nm</td><td>1 m</td></tr>
<tr><td>10^{-2} nm</td><td>10 m</td><td rowspan="8">Radio Waves
(MHz, kHz)</td></tr>
<tr><td>10^{-1} nm</td><td rowspan="3">X-Rays (Å)</td><td>100 m</td></tr>
<tr><td>1 nm</td><td>1 km</td></tr>
<tr><td>10 nm</td><td>10 km</td></tr>
<tr><td>100 nm</td><td rowspan="2">Ultra-Violet (nm),
Visible, Near Infra-Red(μ)</td><td>100 km</td></tr>
<tr><td>1 μ</td><td>10^3 km</td></tr>
<tr><td>10 μ</td><td>Thermal Infra-Red (μ)</td><td>10^4 km</td></tr>
<tr><td>100 μ</td><td>Far Infra-Red (μ)</td><td>10^5 km</td></tr>
</table>

Note: 1 nm (nanometre) = 10^{-9} m and 1 μ (micrometre or micron) = 10^{-6} m

Table 1.1.1.2 Wavelength Range of Visible Colours.

Colour	Wavelength	
	(nm)	(μ)
Violet	380-430	0.38-0.43
Indigo	430-500	0.43-0.50
Blue	500-520	0.50-0.52
Green	520-565	0.52-0.565
Yellow	565-590	0.565-0.59
Orange	590-625	0.59-0.625
Red	625-740	0.625-0.740

The seven colours of the visible spectrum are identified by their wavelengths (Table 1.1.1.2). Radiation of wavelengths shorter than violet is called ultra-violet (UV) radiation. This has very high energy that can break chemical bonds, ionize molecules, damage skin cells or cause cancer. However, most of the UV radiation coming from the sun is absorbed by the layer of atmospheric ozone which resides in the stratosphere, and shields life on earth from its harmful effects.

X-rays have wavelengths that are even shorter than UV, which are expressed in Å (Angstrom Units or 10^{-10} m). Gamma rays have wavelengths that could be as short as 10^{-15} m and it is more convenient to express their magnitude in terms of their energy levels which are of the order of KeV (Kilo electron volts) or MeV (Million electron Volts). X-rays and gamma rays have great penetration power and have applications in astronomy, radioactivity, medicine, and other fields.

Towards the other end of the visible spectrum, radiation which has wavelength higher than red is called infra-red (IR). The IR region of the spectrum can be further sub-divided into near (NIR), short-wave (SWIR), middle (MIR), and thermal (TIR) with increasing wavelength.

Radiation with still longer wavelengths is known by different names such as millimetre waves, microwaves and radio waves. These again are further classified with respect to their frequency as given in Tables 1.1.1.3 and 1.1.1.4.

Table 1.1.1.3 Nomenclature of Microwave and Radio Wave Frequencies.

Abbreviation	Full Form	Frequency	Wavelength
EHF	Extremely high frequency (Microwaves)	30-300 GHz	1 mm-1 cm
SHF	Super high frequency (Microwaves)	30-3 GHz	1 cm-10 cm
UHF	Ultra-high frequency	3 GHz-300 MHz	10 cm-1 m
VHF	Very high frequency	300-30 MHz	1 m-10 m
HF	High frequency	30-3 MHz	10 m-100 m
MF	Medium frequency	3 MHz-300 kHz	100 m-1 km
LF	Low frequency	300-30 kHz	1-10 km
VLF	Very low frequency	30-3 kHz	10-100 km
VF	Voice frequency	3 kHz-300 Hz	$100\text{-}10^3$ km
ELF	Extremely low frequency	300-30 Hz	$10^3\text{-}10^4$ km

Table 1.1.1.4 Microwave Bands.

Band	Wavelength	Frequency
mm-Band	1-7.5 mm	40-300 GHz
Ku-K-Ka- Band	0.75-2.5 cm	12-40 GHz
X-Band	2.5-4 cm	8-12 GHz
C-Band	4-8 cm	4-8 GHz
S-Band	8-15 cm	2-4 GHz
L-Band	15-30 cm	1-2 GHz

1.1.2 Absorption, Emission, Reflection and Scattering

It is quite a paradox that the radiative and thermal equilibrium of the earth-atmosphere system is not controlled by the two major constituents of the atmosphere which are nitrogen and oxygen, but by a few of the numerous miscellaneous gases that all put together make up for just 1% of its volume. The behaviour of gases like water vapour, carbon dioxide, ozone, methane and other trace gases, and also particulate matter floating in the atmosphere, is what alters the radiation from the sun traversing the atmosphere and the radiation returned to space by the earth. Since satellite remote sensing is essentially the measurement of the returned radiation, it is important to know how the gases in the atmosphere influence the radiative processes in the atmosphere.

Atoms and molecules in a gas have electronic, rotational or vibrational energy, and absorption or emission of radiation takes place when there is a transition from one energy state to another. Absorption spectra of atoms, such as atomic oxygen and nitrogen, are associated with electronic transition and occur in the ultra-violet (UV) region of the electromagnetic spectrum. Tri-atomic molecules like those of water vapour, carbon dioxide and ozone, have additional rotational and vibrational transitions, which occur mainly in the infra-red (IR) region. In the visible (VIS) region, gases in the atmosphere account for very little absorption. The main absorption bands are those of three atmospheric gases: water vapour at 6.7 μ, carbon dioxide 15 μ and ozone 9.6 μ (1 μ or micron = 10^{-6} m). There are other minor absorption bands attributable to methane, nitrous oxide, and other gases.

Radiation from the sun gets reflected when it strikes a plane surface such as the ground or cloud tops and its direction gets altered. Depending upon the albedo or reflectivity of the surface, some part of the radiation will be reflected and the remaining amount will get absorbed by the medium or be transmitted through it. Snow and cumulonimbus cloud tops have high albedo values while the ocean surface reflects very little of the radiation falling on it.

Air molecules and suspended particles or aerosols scatter radiation in the VIS wavelengths. When the size of the scattering particles is small compared

to the wavelength of the incident radiation, the scattering is said to be of the Rayleigh type. In Rayleigh scattering, the intensity is inversely proportional to the fourth power of the wavelength, and the distribution of scattered radiation intensity is symmetric in both the forward and backward directions. When the sizes of the scattering particles become comparable to the wavelength of the incident radiation, the scattering processes is said to be of the Mie type, in which the angular distribution of the scattered radiation intensity is complex and asymmetric. Rayleigh scattering by air molecules is what gives the blue colour to the sky, while Mie scattering by the larger sized particles and aerosols gives it a grayish appearance.

1.1.3 Black Body and Radiation Laws

Many fundamental laws governing the absorption and emission of electromagnetic radiation are commonly based on the concept of what is termed as a black body. This is largely a theoretical concept as an ideal or perfect black body can be said to be almost non-existent in reality. A black body is defined as an object that absorbs all radiation incident upon it, does not reflect any of it, and emits all energy at full efficiency for all wavelengths as per the following equation

$$B(\lambda,T) = 2hc^2\lambda^{-5} / (e^{hc/\lambda kT} - 1)$$

where B is the energy in w m^{-2} μ^{-1},
T is the temperature of the black body in ºK,
λ is the wavelength in μ,
h is Planck's constant 6.625×10^{-27} erg sec,
k is Boltzmann constant 1.38×10^{-16} erg $ºK^{-1}$,
c is the velocity of light 3×10^{10} cm sec^{-1}

This relationship of the black body emission to its temperature is known as Planck's Law. For any given temperature, Planck's Law gives a distribution of emitted energy or a characteristic spectrum of electromagnetic radiation that peaks at a certain wavelength. This peak shifts to shorter wavelengths for higher temperatures and the area under the curve grows rapidly with increasing temperature.

Wien's Displacement Law describes the temperature dependence of the black body radiation curves derived from Planck's Law and it states that the wavelength λ_{max} at which the black body radiation is the maximum is inversely proportional to the temperature T of the black body (in ºK), or

$$\lambda_{max} = c / T$$

where c is a constant whose value is 2898 μ ºK.

Stefan-Boltzmann's Law gives the total energy E emitted at all wavelengths by the black body at temperature T,

$$E = \sigma T^4$$

where σ is the Stefan-Boltzmann constant which has a value of 5.6705×10^{-5} erg cm^{-2} sec^{-1} $ºK^{-4}$.

E is in fact the area under the Planck's Law curve. Thus, as the temperature of a black body increases, the shift of the peak emission to shorter wavelengths is governed by Wien's Law while the increase in the height of the curve is explained by Stefan-Boltzmann's Law. This increase in E with temperature is not linear, since it varies with the fourth power of the temperature.

There is another important law called Kirchhoff's Law which states that the ratio ε of emitted radiation to absorbed radiation is the same for all black bodies at the same temperature. This law forms the basis for the definition of emissivity. The emissivity of a perfect black body is 1 and that of a perfect reflector is 0. Strictly speaking, the laws mentioned above are applicable only to a black body, but they are important in the real world as they can be applied as a close approximation to other bodies which have a very weak interaction with the surrounding environment and can be considered to be in a state of equilibrium. In the earth-atmosphere system, the oceanic surface and tall dense clouds can be regarded as acting very similar to a black body.

1.1.4 Solar and Terrestrial Radiation

The radiation laws described in the previous section help us to understand the nature of an object and identify some of its thermal properties by interpreting the pattern of radiation emitted by it in different wavelengths. The spectrum of the solar radiation received at the top of the earth's atmosphere matches very well the spectrum of a black body having a surface temperature of about 5700 ºK. This is called solar radiation and it has a peak at about 0.5 μ (Figure 1.1.4.1). The radiation emitted by a black body at the same temperature as the average temperature of the earth's surface which is 283 ºK, peaks at about 10 μ (Figure 1.1.4.2). We therefore have to deal with two different radiation regimes, the radiation received by the earth from the sun, called solar or shortwave radiation and the radiation returned to space by the earth-atmosphere system, called terrestrial or infra-red or longwave radiation. The intensity of terrestrial radiation is far less than that of solar radiation.

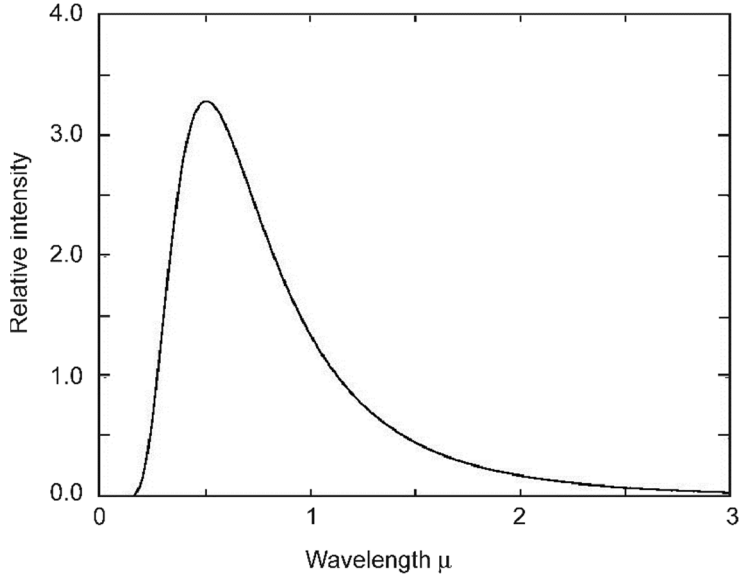

Figure 1.1.4.1 Variation of the relative intensity of black body radiation with wavelength (μ) at temperature 5700 °K, peaking at a wavelength of 0.5 μ in the visible region (Solar radiation).

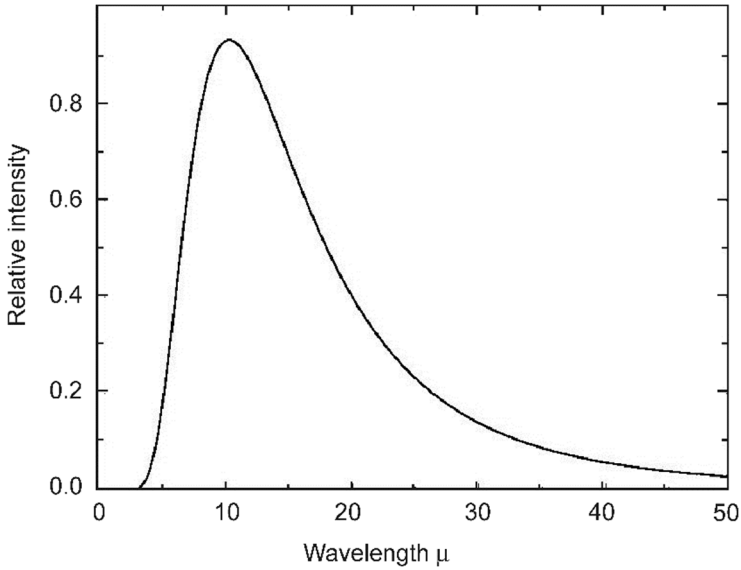

Figure 1.1.4.2 Variation of the relative intensity of black body radiation with wavelength (μ) at temperature 283 °K, peaking at a wavelength of 10 μ in the infrared region (Terrestrial radiation).

1.1.5 Sun-Earth-Atmosphere Radiation Budget

The solar constant is defined as the annual average solar radiation received outside the earth's atmosphere on a plane normal to the incident radiation at the mean sun-earth distance and has a value close to 2 cal cm^{-2} min^{-1} or 1370 W m^{-2}. The actual solar irradiance varies by 3-4% of this value during the year due to the eccentricity of earth's orbit about the sun.

If we consider the incoming solar radiation at the top of the atmosphere as made of 100 units, 30 units are reflected back to space (6 by the atmosphere, 20 by clouds and 4 by the earth's surface). 19 units are absorbed by the atmosphere (16 by gases and 3 by clouds). The remaining 51 units are absorbed by the earth's surface.

Out of these 51 units, 6 are lost to space directly and 45 are returned upwards and absorbed by the atmosphere and clouds (7 by convection and conduction, 23 by evaporation as latent heat and 15 by longwave radiation). The atmosphere and clouds have already absorbed 19 units from the solar radiation, making a total of 64 units which are returned to space as longwave radiation. The budget is thus balanced at the top of the atmosphere.

At the earth's surface and at any level in the atmosphere, the net radiation is the balance of four radiative fluxes, downward solar radiation, downward longwave radiation, upward solar radiation and upward longwave radiation. These can be measured with special instruments installed on the ground or flown on balloons as radiometersondes. The prime factors involved in the radiation budget of the earth-atmosphere system are the albedo or reflectance properties of land, ocean and cloud tops, scattering properties of aerosols, dust and particulate matter in the atmosphere, and vertical profiles of temperature and concentration of gases which absorb longwave radiation (water vapour, CO_2, ozone). Data on these variables if available can be used to compute the radiation budget components indirectly.

1.2 Satellite Orbits

The design of an optimum orbit around the earth for a meteorological satellite is a complex process. There are two main classical types of orbits, polar and geostationary, which are complementary to each other. However, over time, many other types of orbits have come into use or have been tried. The following sections describe the fundamental principles behind orbit design, technical considerations and the operational implications.

1.2.1 Gravitational and Astronomical Laws

There are certain classical laws that were originally formulated to explain the motion of planets in the solar system and their orbits around the sun. They are,

however, very fundamental and general in nature and we now know that they are equally applicable to moons in the solar system or the orbits of artificial satellites placed around the earth and other planets.

Kepler's laws of motion state that: (i) A planet moves around the sun in an elliptical orbit, with the sun at one focus, (ii) The vector joining the sun's centre to the planet sweeps out equal areas in equal time, and (iii) The square of the period of revolution of the planet is proportional to the cube of its semi-major axis. As mentioned above, these laws also hold good for artificial satellites orbiting the earth.

Kepler's laws have to be considered in conjunction with another fundamental physical law. As per Newton's law of gravitation, the gravitational force between two bodies of mass m_1 and m_2 is proportional to the product of m_1 and m_2 and inversely proportional to the square of the distance r between them, or

$$F = G\, m_1\, m_2 / r^2$$

where G is the universal gravitational constant having a value of 6.67×10^{-8} $cm^3\, g^{-1}\, sec^{-2}$.

The forces acting on a satellite around the earth are the gravitational force and the centripetal force, which should balance for the satellite to attain a stable orbit. So we must have

$$m_s\, v^2 / R = GM_e m_s / R^2$$

where M_e and m_s are the masses of the earth and satellite respectively, R is the mean distance between them and v is the velocity of the satellite. The term m_s appears on both sides of the equation and can be cancelled out. We then have

$$v^2 = GM_e / R$$

For a circular orbit, the velocity v can be expressed as $2\,\pi\, R / T$ where T is the time period of revolution of the satellite, which is inversely related to its mean distance from the earth and is given by the equation

$$T^2 = 4\,\pi^2\, R^3 / GM_e$$

This means that the time period, speed and acceleration of an artificial satellite orbiting the earth are not dependent upon its mass. So theoretically speaking we can put into orbit as big a satellite as we wish, the only practical constraint being that of lifting it into space with the rockets that we have.

It needs to be clarified here that the centripetal force is not independent but derived from the continuous gravitation-related fall of the satellite. However, that does not mean that the gravitational force can on its own sustain the satellite stability. Orbits begin to decay slowly with time and the imbalance of forces may need to be occasionally corrected by firing on-board thrusters.

We can evaluate T for a given R as

$$T = (4 \pi^2 R^3 / GM_e)^{½}$$

R can be expressed as $R_e + h$, where R_e is the radius of the earth and h is the height of the satellite above the earth. For the limiting case of h = 0, and using $M_e = 5.98 \times 10^{24}$ kg, and R_e= 6370 km, T works out to be 84 min. In reality of course it is not possible to have a satellite grazing the earth. For h = 200 km, T will work out to be 88 min. For h = 1000 km, T will be 105 min, and this is a popular choice for meteorological satellites.

If T is set at 24 hr, the height of the satellite will work out to be about 35,840 km above the earth's surface. Such an orbit is called geosynchronous as the satellite matches the angular velocity of the earth at this height.

1.2.2 Orbital Elements

As depicted in Figure 1.2.2.1, the satellite's orbit is specified by the following parameters (Kelkar et al 1980):

(a) a - the semi-major axis of the orbit (defines the size of the orbit)

(b) e - the eccentricity of the orbit (defines the shape of the orbit)

(c) I - the inclination of the orbit (with respect to the earth's equatorial plane)

(d) Ω - the right ascension of the ascending node (longitude of the north-bound equatorial crossing)

(e) ω - the argument of the perigee

(f) f - true anomaly

(g) T_e - epoch time

For a given orbit, all the above parameters are fixed, except f which specifies the position of a satellite at a given time.

The semi-major axis a of the ellipse is the maximum height of the satellite above the earth's surface. As per Kepler's third law, satellites move faster when they are close to the earth and slower when they are further away. The semi-major axis is thus an indirect measure of the average speed or mean motion of the satellite.

The satellite orbit is generally an ellipse. The eccentricity e is an indicator of the shape of the ellipse. A circular orbit is a special case of an ellipse when e is 0, and as e increases towards the limiting value of 1, the ellipse becomes more and more eccentric or elongated.

The point where the satellite is closest to the earth is called the perigee, and the point where it is farthest from the earth is called the apogee. The major axis of the ellipse is thus the line joining the perigee and the apogee. The argument of perigee ω helps to define the orientation of the orbital ellipse within the orbital plane. It is the angle measured at the centre of the earth from the ascending node to the perigee.

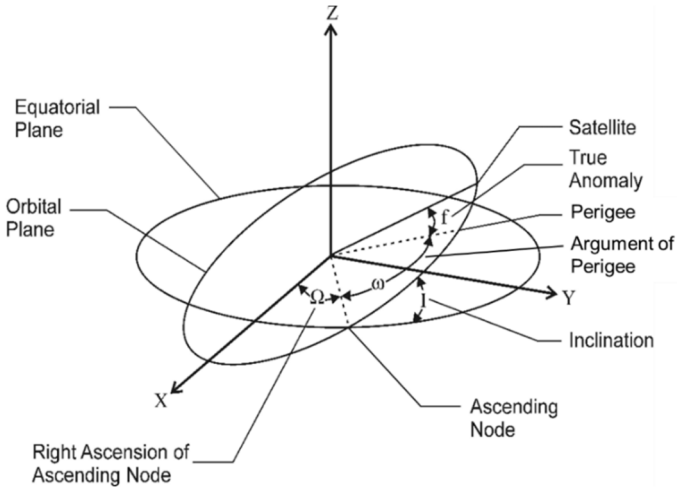

Figure 1.2.2.1 Orbital elements of a satellite in orbit around the earth.

For a given inclination, there can be an infinite number of orbital planes. The intersection of the equatorial plane and the orbital plane is known as the line of nodes. The right ascension of the ascending node along with the inclination uniquely specifies the orbital plane. The ascending node is the longitude at which the satellite crosses the equator while going from south to north. The descending node is where the satellite crosses the equator while going from north to south. Since the earth is spinning, we cannot use the common latitude/longitude coordinate system to specify where the line of nodes points. Instead, we use an astronomical coordinate system, known as the right ascension/declination coordinate system, which does not spin with the earth. Right ascension is an angle measured in the equatorial plane from a reference point in the sky where right ascension is defined to be zero, which is the vernal equinox. Thus the right ascension of the ascending node Ω denotes an angle, measured at the centre of the earth, from the vernal equinox to the ascending node.

The true anomaly f is the angle at the centre of the earth, measured in the orbital plane, between the perigee and the satellite at any given time. If the satellite is in a circular orbit and hence moving at a constant speed, this angle would point directly to the satellite.

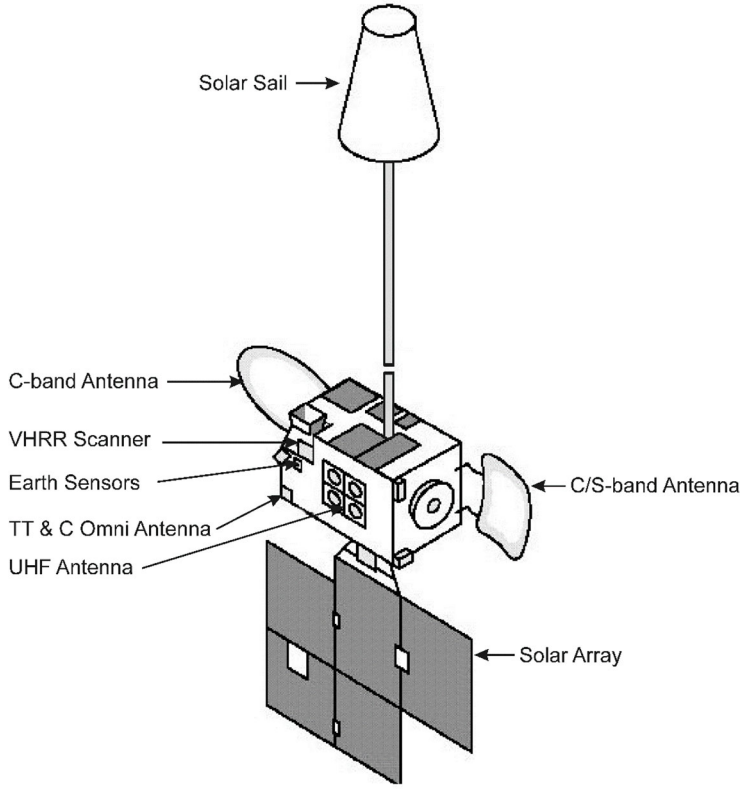

Figure 1.2.2.2 A schematic of the INSAT-1 spacecraft.
(Source: IMD)

A satellite orbit may be subjected to small perturbations due to different reasons such as non-sphericity of the earth's geoid leading to gravitational anomalies, gravitation effects of other celestial bodies like the sun, moon or stars, atmospheric drag, solar radiation pressure and tides. The order of magnitude of these perturbations would depend on the nature of the satellite orbit. For example, geostationary satellites at 36,000 km height would be less prone to atmospheric drag, but more sensitive to the pressure of solar radiation, whereas the reverse would be true in the case of low altitude polar orbiting satellites. Early spacecrafts of the INSAT series had large solar panels on one side and a long solar sail on the other side for balancing the solar radiation pressure (Figure 1.2.2.2).

1.2.3 Types of Orbits

For almost four decades, from TIROS-1 in 1960 to the Tropical Rainfall Measuring Mission (TRMM) satellite in 1997, there were only two preferred orbits for meteorological satellites, polar and geostationary. A polar orbit is typically a circular orbit having an altitude of about 850 km and a period of revolution of about 100 min (Figure 1.2.3.1). This results in the satellite scanning a 3000 km wide swath on the earth's surface. It crosses the equator only twice a day, but views the poles in every orbital revolution. With each successive revolution, a new region of the earth comes under its view because in the meantime the earth has rotated around its own axis. The satellite completes 14 orbits in a day, so a global montage of images can be constructed over a period of 12 or 24 hr.

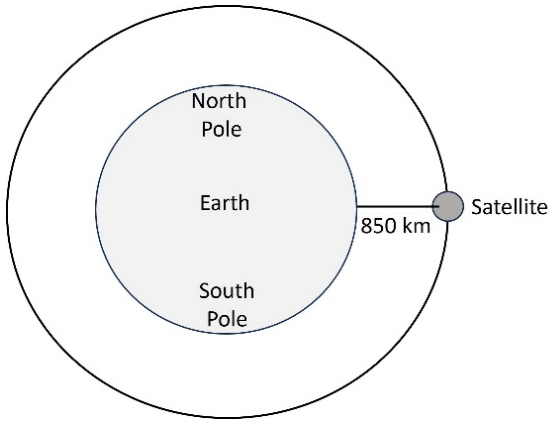

Figure 1.2.3.1 Polar orbit.

The earth is not a perfect sphere and the surface mass is not uniformly distributed all over, leading to gravitational anomalies. Other bodies in the solar system also exert their gravitational influence on a spacecraft in orbit around the earth. It is possible, however, to use these factors to advantage and induce precession or a slow movement of the satellite orbital plane with respect to the fixed inertial space. A special type of a polar orbiting satellite is a sun-synchronous satellite which is designed in such a manner that the precession of the satellite orbit matches the earth's revolution around the sun. The result is that the satellite crosses a place on the equator at the same local time (there are AM and PM orbits) and views it under comparable lighting conditions. The orbit does not go exactly over the poles but needs to have an inclination of about 99 or 100º. Occasional orbit manoeuvres may be required to maintain the sun-synchronous characteristics of the orbit.

When a satellite is placed in a circular orbit with a radius of 42,400 km or a height of 36,000 km above the earth's surface, it will circle round the earth with the same angular velocity as that of the earth. At that specific height, it will complete one orbital revolution around the earth in 24 hours. Such a satellite is called a geosynchronous satellite (Figure 1.2.3.2). If its orbit lies in the earth's equatorial planet it will appear, in a relative sense, to remain stationary above a given point on the equator. Such a satellite is called a geostationary satellite and it can provide a continuous earth view. Practically, however, the useful view is limited to about 60º around the subsatellite point, as the image outside it gets distorted. A constellation of 5 or 6 geostationary satellites spaced around the equator can together give a near-global picture. Geostationary satellites are ideal for communications purposes and continuous monitoring of the weather over the region within their view. Considerations of orbit stability demand that a geostationary satellite be placed only over a point on the equator and not above any other latitude. To maintain the geostationary satellite within the nominal limits of altitude and inclination, station-keeping manoeuvres have to be carried out periodically.

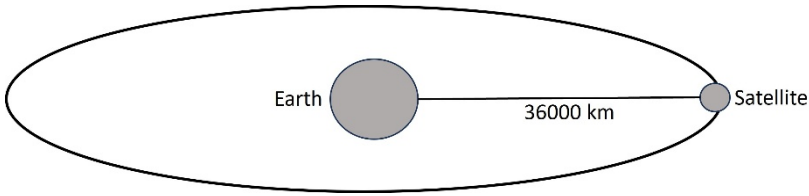

Figure 1.2.3.2 Geostationary orbit.

When the direction in which a satellite is moving in its orbit around the earth is the same as that of the rotation of the earth, the orbit is called direct or prograde. If the satellite is moving in a direction that is opposite to that of the earth's rotation, the orbit is called retrograde. A geostationary satellite orbit is generally prograde and a polar orbit generally retrograde.

Kelkar et al (1982) had envisaged a low-altitude non-geostationary satellite that would orbit around the equator and provide frequent meteorological coverage of the entire tropical belt. In the years that followed, many such orbits with different inclinations have become a reality. In 1997, TRMM was launched into an orbit having 35° inclination and in 2011, Megha-Tropiques in a 20° inclined orbit. In 2014, the GPM core satellite went into a 65° inclination orbit and in 2023, TROPICS into a 30° inclination orbit. These missions are described in later chapters. The orbital inclinations of these satellites are shown schematically in Figure 1.2.3.3.

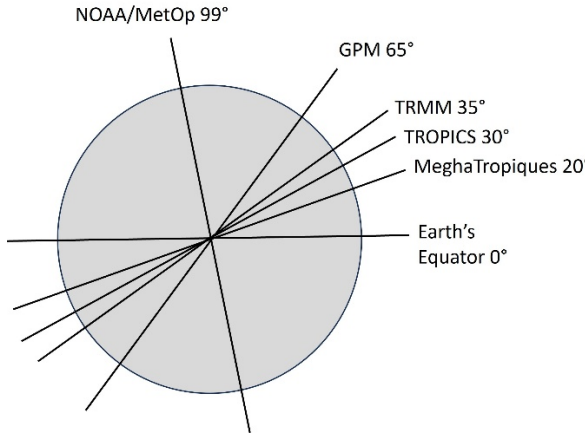

Figure 1.2.3.3 Orbital inclinations of various satellites.

While geostationary meteorological satellites provide continuous coverage of the earth, they have many basic constraints that simply cannot be overcome. For a geostationary satellite to be stable, its orbit must ideally lie in the earth's equatorial plane. Its subsatellite point can only be on the equator and over no other latitude. So one cannot have a satellite positioned over say, New Delhi or New York. With more countries launching their own geostationary satellites, the already crowded equatorial parking space is also going to come under greater stress.

A ingeniously designed orbit that combines the advantages of both polar and geostationary orbits is known as the Molniya orbit and between 1965 and 2004, several Russian satellites were launched into it. An ideal geostationary orbit must be perfectly circular, that is its eccentricity should be zero. In contrast, a Molniya orbit is by definition highly eccentric. Its perigee is about 400 km like that of a low earth orbit satellite and its apogee is of the order of 40,000 km like a geostationary satellite (Figure 1.2.3.4). Its orbital period is about 12 hr. In accordance with Kepler's second law, a spacecraft in a Molniya orbit would remain for a long time in the vicinity of the apogee. If the apogee is above a polar region, then a long continuous view of the polar region can be obtained.

The Molniya satellites were used mainly for purposes like communications and their application to meteorology remained limited. Another constraint was that spacecrafts in a Molniya orbit had to pass through the earth's Van Allen radiation belts repeatedly and therefore needed appropriate radiation shielding. Currently two Russian Molniya satellites Arktika-M-N1 and -N2, launched in 2021 and 2023 respectively, are operational and a new Molniya satellite series named Meridian has also been planned.

The advantages of having two or three satellites in highly elliptic orbits for observing the polar regions have been discussed in detail by Trishchenko et al (2019).

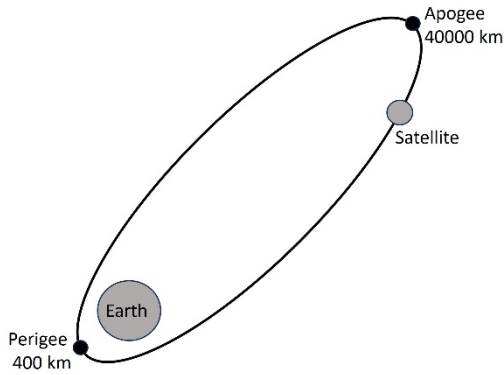

Figure 1.2.3.4 Highly elliptical Molniya orbit.

Around the beginning of the new millennium, the World Meteorological Organization (WMO) had mooted the concept of an International Geostationary Laboratory (IGeoLab). This called for a partnership among various countries that would allow geostationary meteorological satellites to be moved around to different locations on the equator as required, either for demonstration missions or for operational reasons (Hinsman 2006). A major logistical challenge to the exercise, however, was the non-availability of a sufficient number of the equatorial slots. While there was a strong interest in the meteorological satellite community, the IGeoLab project did not eventually materialize for various reasons. One of the missions proposed under the IGeoLab programme, was the Geostationary Imaging Fourier Transform Spectrometer (GIFTS). This was a new measurement concept that combined several advanced technologies, providing high vertical resolution temperature and moisture soundings (Smith et al 2002). This too showed much promise but did not make enough headway.

1.2.4 Satellite Attitude

While the altitude of a satellite is its height above the earth, the term satellite attitude refers to its orientation in space. Altitude and attitude are two equally important characteristics of a satellite and they together determine the kind of mission that the satellite can best perform. In the case of a meteorological or remote sensing satellite, the antennas must always remain in ground contact for communications and data transfer, and its imaging sensors must always view the earth as intended. Any deviation from the nominal attitude would

result in an improper functioning of the satellite. Satellite attitude therefore demands to be carefully controlled and the two ways of doing it are through spin-stabilization and three-axes stabilization.

A spin-stabilized satellite rotates around its own vertical axis, spinning like a top and resisting external perturbation forces. Here the orientation of the satellite spin vector in space defines its attitude. Spin-stabilized satellites are equipped with thrusters which can be fired occasionally to bring about desired changes in the spin rate and to restore the spin vector orientation. The early geostationary satellites had a cylindrical design and rotated at the rate of one revolution per second during which the earth's disc would be scanned. A disadvantage in spinning satellites is that they cannot have large solar arrays and require to be supported by battery power. Another inconvenient factor is that instruments or antennas are required to de-spin so that the antennas and radiometers maintain their desired orientation relative to the earth.

The first Indian National Satellite, INSAT-1A, launched in 1982, was different from the U. S. and European geostationary satellites operating at that time, in that it was a non-spinning satellite, a design that was later adopted by many other countries including the U. S. In a non-spinning satellite, the attitude is defined in terms of the deviations from the nominal orientations of its roll, pitch and yaw axes. The terms roll, pitch and yaw are applied to a satellite in the same manner as they are used in the case of sailing ships or aircrafts in flight. Roll is the rotation of the spacecraft around the direction of its forward movement. Yaw is its rotation around the axis looking at the nadir. Pitch is the rotation around an axis normal to the roll and yaw axes. The three axes can be envisaged as lines running through the satellite's centre of gravity and intersecting at right angles (Figure 1.2.4.1).

The attitude of a non-spinning satellite is controlled by minimizing the roll, pitch and yaw. This is called three-axes stabilization, and achieved through the deployment of electrically powered spinning wheels called momentum or reaction wheels. These wheels are mounted in three orthogonal axes on the spacecraft and allow a transfer of angular momentum back and forth between the spacecraft and wheels. If the satellite is found to be deviating from its desired attitude, the appropriate spinning wheels are speeded up or slowed down to restore the correct attitude. Spacecrafts may also have propulsion system thrusters to apply the required torque. An advantage of three-axes stabilization is that radiometers and antennas can always be made to point at the desired targets without having to perform de-spin manoeuvres.

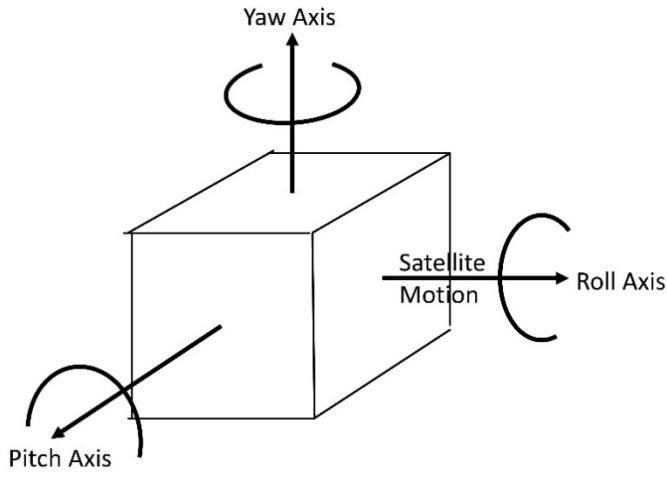

Figure 1.2.4.1 Roll, pitch and yaw axes of a satellite.

In three-axes stabilized geostationary meteorological satellites, the scanning radiometers have to alternate their scans between east-west and west-east directions until the earth's disc gets fully scanned. The polar-orbiting NOAA satellites are also three-axes stabilized but the scanning is required to be done only in the east-west direction as the north-south progression of the scan is taken care of by the movement of the satellite in its orbit.

Attitude errors result in a distortion of the satellite image and the scene viewed looks slightly different from the nominal view. Yaw errors will result in the image getting rotated around the sub-satellite point in a clockwise or anticlockwise manner. With roll and pitch errors, the image will not be centred at the nominal sub-satellite point but a little away from it. When the attitude errors are large, the sub-satellite point of a geostationary satellite is seen to meander in a figure-of-eight pattern around its nominal position on the equator.

1.3 Meteorological Satellite Payloads

The basic payload carried by the first ever meteorological satellite in 1960 was just a television camera that relayed to the ground whatever it saw of land, ocean and clouds. With every successive meteorological satellite launched over the last six decades by different countries, there have been rapid advances in satellite instrumentation and technology, serving various areas of application, which will be described in the next few sections and the following chapters of this book.

1.3.1 TV Cameras

Historically speaking, the earliest attempt to observe the earth's weather from space was made by the U.S. satellite, Vanguard 2, which was launched on 17 February 1959 but it could not collect much useful data. The world's first meteorological satellite to be considered a success, was the Television and Infra-Red Observation Satellite, TIROS-1, which was launched by the U. S. on 1 April 1960. TIROS-1 was operational for only 78 days, but it demonstrated beyond doubt the tremendous potential use of satellites for surveying global weather conditions from space and paved the way for future advancements.

TIROS-1 had carried two television cameras, a low-resolution one and a high-resolution one. The pictures were transmitted directly to ground receiving stations. Each camera had a magnetic tape recorder for storing photographs taken when the satellite was out of range of ground stations. The spacecraft was spin-stabilized but not earth-oriented. Therefore, the cameras were only operated while they were pointing at the earth when that portion of the earth was in sunlight. The video systems relayed thousands of pictures containing cloud cover views of the earth that provided information about large scale cloud regimes for the first time.

Many more satellites in the TIROS series were launched thereafter. TIROS-8 launched in December 1963 was the first satellite to be equipped with the Automatic Picture Transmission (APT) capability that made satellite pictures available the world over to meteorological agencies in real time as the satellite passed over their region. For this purpose, 50 ground stations were established, including one at Mumbai (Colaba) in India (Datar et al 1971),

The successor satellite programme was named after the U.S. agency, the Environmental Science Services Administration (ESSA), which operated it. The ESSA series was initiated in 1966 as an extension of the TIROS programme and its primary objective was to acquire higher resolution cloud cover images. Over the next four years, nine satellites in the ESSA series transmitted thousands of images that helped to predict weather patterns including hurricanes. By the end of the programme, more than 300 APT reception stations had come up in 45 countries.

In 1964, the U.S. National Aeronautics and Space Administration (NASA) launched a parallel satellite programme named Nimbus, to develop observation systems aimed at meeting the research requirements of atmospheric and earth sciences. Between 1964 and 1978, NASA launched seven Nimbus satellites which had very advanced on-board instruments for mapping ozone, sea ice, radiation budget components, coastal zone properties and sea surface temperature, However, Nimbus satellites also continued to

carry an improved vidicon camera system for daylight coverage of local cloud conditions which were transmitted through the APT system.

A similar APT service was provided parallelly by the Russian Meteor series of satellites. However, the early satellites in this series were not sun-synchronous and the images were received at different times of the day in each pass.

1.3.2 Scanning Radiometers

After the end of the TIROS satellite series, TV cameras were given up and replaced by scanning radiometers which have since became more and more advanced. Scanning radiometers do not take snapshot pictures of the earth's surface and clouds but they scan them and measure the radiation received from them. In spin stabilized satellites, the rotation of the satellite about its spin axis provides the east-west sweep of the detectors. In 3-axes stabilized satellites, the detectors have to alternately perform east-west and west-east scans. The north-south scan is achieved in mechanical steps.

The digital data so collected is processed on ground and converted into an image format. What the resultant satellite image looks like depends upon the spectral band in which the satellite radiometer has measured the radiation, the sensitivity and response of the sensor, the height from which the satellite is viewing the earth, the time of the scan and such other factors.

The TIROS-N satellite launched by the U.S. in October 1978, carried a 4-channel radiometer known as the Advanced Very High Resolution Radiometer (AVHRR). This was subsequently improved to a 5-channel instrument (AVHRR/2) that was initially carried on the NOAA-7 satellite launched in June 1981. The AVHRR/3 with 6 channels was first carried on NOAA-15 in 1998. Details of the 6-channel NOAA AVHRR/3 are given in Table 1.3.2. The spectral bands are window regions of the spectrum and are so chosen as to allow maximum amount of radiation to reach the satellite. Most subsequent polar orbiting and geostationary satellites have continued with a similar or expanded version of this basic channel configuration in their scanning radiometers.

Details of the Very High Resolution Radiometer (VHRR) instrument on successive INSAT satellites are summarized in Table 1.6.1. The design and functioning of the INSAT INSAT-2A and -2B VHRR instrument have been described by Joseph et al (1994), further improvements and additions made to the INSAT-2E VHRR by Iyengar et al (1999) and the far more sophisticated INSAT-3D imager operations by Mohapatra et al (2021).

Table 1.3.2.1 NOAA AVHRR/3 Channels.

Channel Number	Spectral Band	Wavelength Range (μ)	Applications
1	VIS	0.58 - 0.68	Daytime cloud and surface mapping
2	NIR	0.725 - 1.00	Land-water boundary delineation
3A	NIR	1.58 - 1.64	Snow and ice detection
3B	MIR	3.55 - 3.93	Night-time cloud mapping, sea surface temperature retrieval
4	TIR	10.3 - 11.3	Night-time cloud mapping, sea surface temperature retrieval
5	TIR	11.5 - 12.5	Sea surface temperature retrieval

1.3.3 Sounders

The most widely used instrument for measuring pressure, temperature and humidity at various levels in the atmosphere is the radiosonde. This is an electronic package of sensors and a transmitter that is attached to a balloon. As the balloon rises, the signals received at a ground station are decoded to obtain the vertical profiles of temperature, humidity and other parameters. Most upper air stations take two radiosonde ascents per day at the synoptic hours of 00 and 12 UTC. With the advent of satellites, sounders were designed to do what radiosondes did. Satellite-based soundings had several advantages like they did not need consumables such as balloons, gas and electronics, and they could be done frequently and at more grid points.

In 1979, the NOAA-6 satellite first carried an instrument called the TIROS Operational Vertical Sounder (TOVS) which in fact consisted of three separate parts: High Resolution Infra-red Radiation Sounder Version 2 (HIRS/2), Microwave Sounding Unit (MSU) and Stratospheric Sounding Unit (SSU). The system as a whole provided atmospheric temperature profiles from the surface to 10 hPa, water vapour content at three levels of the atmosphere and total ozone content. The HIRS/2 was a step-scanner 20-channel spectrometer with 19 IR channels and one VIS channel (Smith et al 1979). Sounders came into wide use subsequently in several orbiting and geostationary satellites.

In principle, a satellite sounder instrument makes radiance measurements in the absorption bands of CO_2 centred at 15 and 4.3 μ, water vapour at 6.7 μ and ozone at 9.6 μ. Sampling at the centre of the band yields radiation from the upper levels of the atmosphere, as radiation from below has already been absorbed by the atmospheric gas. Sampling away from the centre of the absorption band yields radiation from successively lower levels of the atmosphere. Details of the retrieval process will be described later in the next chapter.

The current INSAT-3D satellites are also equipped with a 19-channel sounder. The sounder has 18 narrow spectral channels in shortwave infrared, middle infrared and thermal infrared regions and one channel in the visible region. The ground resolution at nadir is nominally 10 km for all nineteen channels. The instrument can make soundings at 10 km ground resolution every 3 hours for a full frame scan. Derivation of vertical profiles of temperature and humidity over 30 x 30 km areas is possible. Besides these vertical profiles, there are many other parameters than can be derived such as atmospheric stability indices, total precipitable water, and total column ozone.

1.3.4 CCD Imagers

While Charge Coupled Devices (CCDs) were widely used much earlier in remote sensing satellites for land resources applications, India was the first country to fly a 3-band CCD-based imager in geostationary orbit on its INSAT-2E satellite to complement the VHRR. A similar instrument was also flown on the INSAT-3A satellite. It provided co-registered images of the earth in VIS (0.62-0.68 μ), NIR (0.77-0.86 μ) and SWIR (1.55-1.69 μ) regions of the spectrum. The ground resolution of these images at the sub-satellite point was 1 km for all the three bands. The spectral bands as well as dynamic range and saturation radiance set points were so selected that the images could be used for meteorological applications as well as vegetation mapping and other earth resources applications.

The CCD imager was similar to the VHRR as far as the basic telescope design and scan mechanism were concerned. The separation of the three bands was achieved by two dichroic beam splitters. This optical configuration was designed for achieving identical footprints on the ground while accommodating two different sizes of detector elements. Flexible programmable scan modes allowed generation of images with up to 24 contiguous strips covering an area of 6300 × 6300 km on earth. Again, a positioning mechanism enabled this image field to be positioned anywhere in a scan field of 20º × 20º covering the full earth disc.

A complete technical description of the INSAT CCD imager has been given by Iyengar et al (1999), while Padmanabhan et al (2004) have discussed the complex nature of the CCD image processing. Bhatia et al (1999) have described the wide variety of applications possible with the fine resolution and continuous temporal coverage provided by the INSAT CCD imager.

1.3.5 Multispectral and Hyperspectral Imaging

The spectral resolution of a satellite sensor is inversely related to the spectral range covered by it. A higher spectral resolution and an accurate spectral signature can be obtained by having a large number of narrow bands, rather than one continuous broad band. Further, the spectral resolution and spatial

resolution are also inversely related, since for registering the small amount of radiance contained in a very narrow spectral band, the sensor must dwell on the ground area for a longer time. However, if the satellite sensors are made to scan the earth at a slow speed they will take longer to complete the scan, thus reducing the temporal resolution or repetivity of observations as well. Remote sensing satellites can have a long repeat cycle of 10-20 days and can therefore make measurements in narrow spectral channels. Meteorological satellites cannot do this and in order to accomplish fast earth scans, they acquire stronger radiances from wider spectral bands such as VIS 0.55-0.75 μ or TIR 10.5-12.5 μ. The sensor response is, however, not uniform over the entire width of the channel and even if many satellite radiometers have nominally the same spectral bandwidths, their spectral response functions across the band are not identical. This is the reason why images of the same region obtained from different satellites look a little different from each other.

Precision spectroradiometers are usually based on a monochromator with a diffraction grating. A concave mirror collimates the radiation and the diffraction grating reflects the radiation while dispersing it into its spectral components. A second concave mirror focusses the radiation on a detector. Scanning of the spectrum is accomplished by rotating the grating while recording the electrical signal at the detector.

A satellite-based spectroradiometer can provide extremely high spectral sensitivity with exceptionally low out-of-band response. One such instrument called the Moderate Resolution Imaging Spectroradiometer (MODIS) was flown aboard the Terra and Aqua satellites launched in 1999 2002 respectively by NASA. Terra's orbit around the earth is timed so that it passes from north to south across the equator in the morning, while Aqua passes south to north over the equator in the afternoon.

Table 1.3.5.1 MODIS Spectral Bands and their Applications.

Band	Spectral Range (μ)	Primary Applications
1	0.620 – 0.670	Land/Cloud/Aerosols Boundaries
2	0.841 – 0.876	
3	0.459 – 0.479	Land/Cloud/Aerosols Properties
4	0.545 – 0.565	
5	1.230 – 1.250	
6	1.628 – 1.652	
7	2.105 – 2.155	

Table 1.3.5.1 *Contd….*

Band	Spectral Range (μ)	Primary Applications
8	0.405 – 0.420	Ocean Colour/ Phytoplankton/ Biogeochemistry
9	0.438 – 0.448	
10	0.483 – 0.493	
11	0.526 – 0.536	
12	0.546 – 0.556	
13	0.662 – 0.672	
14	0.673 – 0.683	
15	0.743 – 0.753	
16	0.862 – 0.877	
17	0.890 – 0.920	Atmospheric Water Vapour
18	0.931 – 0.941	
19	0.915 – 0.965	
20	3.660 - 3.840	Surface/Cloud Temperature
21	3.929 - 3.989	
22	3.929 - 3.989	
23	4.020 - 4.080	
24	4.433 - 4.498	Atmospheric Temperature
25	4.482 - 4.549	
26	1.360 - 1.390	Cirrus Clouds Water Vapour
27	6.535 - 6.895	
28	7.175 - 7.475	
29	8.400 - 8.700	Cloud Properties
30	9.580 - 9.880	Ozone
31	10.780 - 11.280	Surface/Cloud Temperature
32	11.770 - 12.270	
33	13.185 - 13.485	Cloud Top Altitude
34	13.485 - 13.785	
35	13.785 - 14.085	
36	14.085 - 14.385	

As of July 2025, both Terra and Aqua were still operational. MODIS views the entire earth's surface every 1 to 2 days, acquiring data in 36 spectral bands ranging in wavelength from 0.4 to 14.4 μ. The responses are tailored to meet the needs of several applications (Table 1.3.5). The resolution at nadir is 250 m for bands 1-2, 500 m for bands 3-7 and 1 km for bands 8-36. A ± 55º scanning pattern at an orbital altitude of 705 km achieves a 2,330 km swath.

Hyperspectral imaging is a powerful means of further reducing the spectral channels to extremely small widths, even as small as 0.01 μ. With such narrow widths, the spectral range from 0.38 to 2.55 μ for example, can be divided into as many as 217 intervals. This is made possible by the use of silicon microchips as detectors for the very near IR region, and Indium-Antimony (In-Sb) alloy detectors for the shortwave SWIR region. The radiance values measured by the CCDs for each such narrow interval are plotted as a graph of intensity versus wavelength, that provides a sufficient number of points through which we a meaningful continuous spectral curve can be drawn. Hyperspectral imaging is in principle far superior to multi-spectral imaging, as it provides much more detail about the spectral properties of the features to be identified. The hyperspectral data yields continuous spectral signatures rather than the band histogram plots.

1.3.6 Passive Microwave Sensors

Seasat, Nimbus-5, Nimbus-7 and India's Bhaskara-II, were the earliest satellites to carry passive microwave radiometers and clearly demonstrated the potential of microwave measurements in the retrieval of atmospheric and oceanographic parameters.

Bhaskara-II, which was launched in 1981, carried a Satellite Microwave Radiometer (SAMIR) that had three channels at 19.35, 22.235 and 31.4 GHz with vertical polarization. The observations were taken close to nadir at angles of 2.8º and 5.6º along the satellite ground trace during each spin of the satellite. The footprint had a size of 240 km. Pathak et al (1992) used SAMIR data for the period January 1982 to June 1983 to derive the latitudinal variation of monthly mean values of atmospheric water vapour content over the Arabian Sea and Bay of Bengal and studied its seasonal and geographical variations. Gohil et al (1982) had earlier derived atmospheric water content from Bhaskara SAMIR data.

Microwave remote sensing, however, took some time to come into wider use. This was because of the weak microwave signal strength, poor ground resolution of microwave images and the high variability of the land surface emissivity in the microwave region. The principles of satellite-borne microwave radiometry have been reviewed by Pandey (1995).

The Defense Meteorological Satellite Programme (DMSP) is a long term U.S. Air Force effort in space to monitor the meteorological, oceanographic

and solar-geophysical environment of the earth. In December 1972, DMSP data was declassified and made available to the civilian and scientific community. The Special Sensor Microwave Imager (SSM/I), was first flown on the DMSP satellites in June 1987. This was a 7-channel, 4-frequency, linearly polarized, passive microwave radiometric system measuring atmospheric, ocean and terrain microwave brightness temperatures at 19.35, 22.235, 37.0 and 85.5 GHz with footprint sizes varying from 13 × 15 km at 85 GHz to 43 × 69 km at 19 GHz.

The TRMM Microwave Imager (TMI) on board the Tropical Rainfall Measuring Mission (TRMM) satellite, launched in 1997, was a passive sensor operating at 5 microwave frequencies of very similar to those of SSM/I. The Indian Remote Sensing Satellite IRS-P4, also known as Oceansat-1, which was launched in May 1999, carried a Multi-channel Scanning Microwave Radiometer (MSMR) operating at 6.6, 10, 18 and 21 GHz frequencies in both H and V polarizations.

Microwave data are now being used to derive a variety of geophysical parameters such as, ocean surface wind speed, ice cover, cloud liquid water, integrated water vapor, precipitation over water, soil moisture, land surface temperature, snow cover and sea surface temperature. Most of the retrieval algorithms in vogue are in the form of statistical correlations between the brightness temperatures of various channels or differences between channels, with these parameters.

1.3.7 Active Sensors

Passive scanning radiometers measure the radiation reaching the satellite from the earth's surface or cloud tops in different wavelength bands including microwave. In active remote sensing, on the other hand, a radar placed on board a satellite emits microwave signals at a certain frequency and then measures the radiation scattered back from the earth's surface or cloud tops. This yields much more information than a passive microwave radiometer would.

However, there are practical issues. For a radar on a geostationary satellite, the range becomes enormous. Polar orbiting satellites move at high speed relative to the earth and the dwell time is insufficient. Therefore, the beam width of the radar has to be narrow enough to be fully filled with precipitation and the swath has to be wide enough to eliminate gaps in coverage. A space-borne radar must also be able to discriminate the weak precipitation echo over the strong return from the earth's surface. Hence it becomes desirable to use wavelengths shorter than 3-10 cm which are used in conventional weather radars on the ground, as at shorter wavelengths the return echo is stronger.

The TRMM Precipitation Radar was the first space-borne radar that was designed specifically to measure rainfall in three dimensions over tropical and subtropical region.

Satellite measurement of cloud properties became a reality with the successful launch of two satellites, CloudSat and CALIPSO, in April 2006. CloudSat carried a mm-wave radar and CALIPSO had on board a backscattering lidar. The pair of satellites formed a unique combination of radar and lidar in space.

1.4 Satellite Imagery

As satellite images started becoming available to meteorologists around the world in the early 1960s, the skills of satellite image interpretation developed very rapidly. Until then, knowledge about clouds had been documented into cloud atlases on the basis of what had been observed from the ground or aircrafts. The view from satellite altitudes was, however, completely new, and clouds seen by satellites had to be interpreted in an altogether different manner.

In the early days of the satellite era, the imaging technology was primitive. APT pictures received directly from satellites flying overhead were produced on facsimile chart paper, mostly of inferior quality and liable to fading in a short time. The images many times lacked clarity and hence they had to be examined with great care. However, the technology improved really fast and even photographic paper was mostly done away with, when interactive computer image processing systems became common. Now of course, there are web sites on the internet and mobile apps on which anyone can access satellite imagery in near real time.

Satellite images are constructed by assigning the measured radiance a certain brightness value usually on a scale ranging from 0 to 255 or from 0 to 1023, which is called the gray scale. The number 0 on the gray scale stands for pure black and the highest number stands for pure white.

In a typical VIS image (Figure 1.4.1), the lowest values on the gray scale are seen over oceans because of their high absorption of solar radiation. The highest gray scale values are seen over snow covered regions and Cb cloud tops, which reflect solar radiation the most. Shallow clouds having low cloud water/ice content and large cloud droplet size have intermediate gray scale values. In an IR image (Figure 1.4.2), the lower end of the gray scale corresponds to high temperatures and the higher end of the gray scale to low temperatures. In a WV image (Figure 1.4.3), lower values of the gray scale correspond to dry regions and higher values to moist regions.

The information derived from the VIS, IR, WV and microwave channels is not redundant but complementary. The most important advantage of IR and WV imagery is that it is available at all times unlike VIS imagery which is available only in daylight hours.

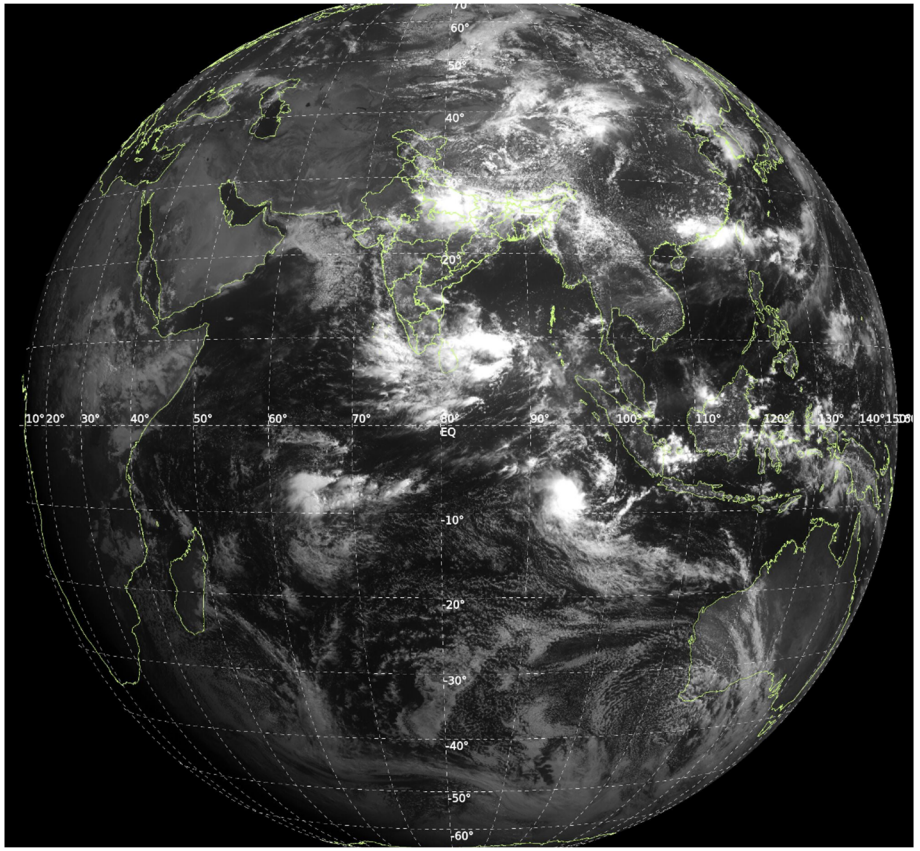

Figure 1.4.1 INSAT-3DS 3 August 2025 0500 UTC VIS full disc image. (Source: https://mausam.imd.gov.in/)

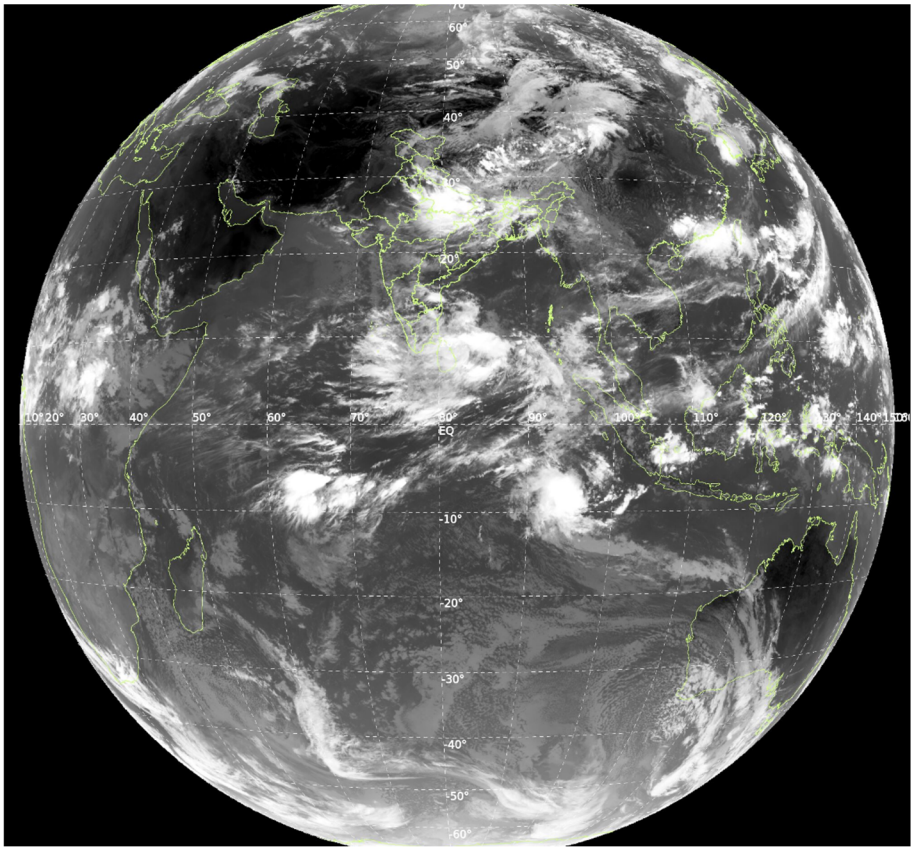

Figure 1.4.2 INSAT-3DS 3 August 2025 0500 UTC TIR1 full disc image. (Source: https://mausam.imd.gov.in/)

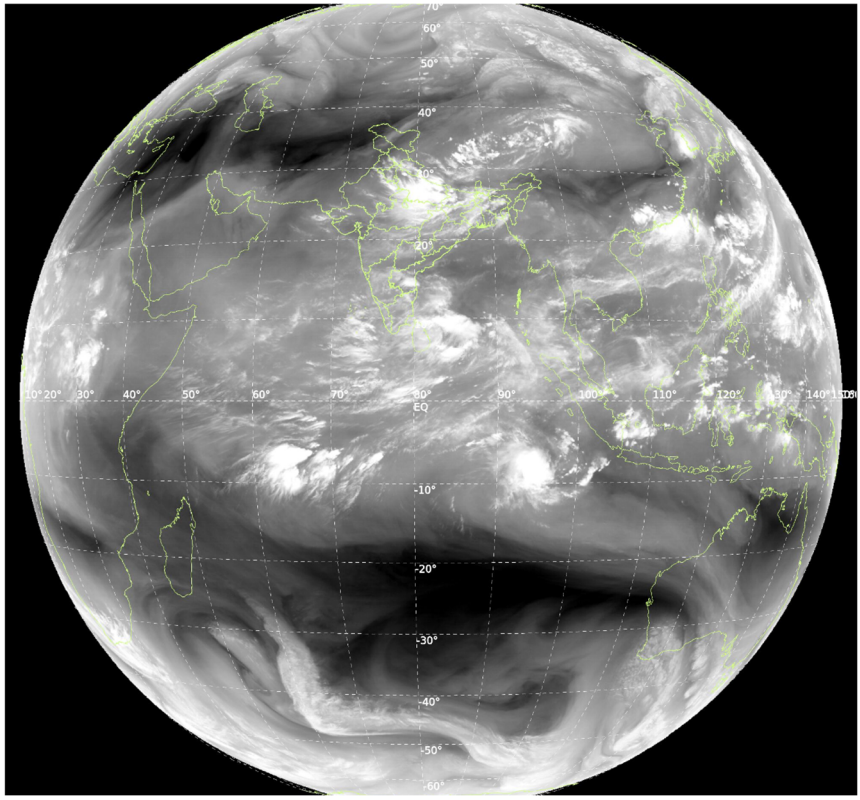

Figure 1.4.3 INSAT-3DS 3 August 2025 0500 UTC WV full disc image. (Source: https://mausam.imd.gov.in/)

1.4.1 Resolution

The term resolution as applied to meteorological satellites assumes a different meaning in different contexts: spatial, spectral, radiometric and temporal, but in each case it is a critical design consideration. While the design aim would be to have the finest resolution, it is not always possible to attain it and what is realized is a trade-off between several competing factors. A higher resolution also requires extremely high rates of data transfer and an increasingly complex design of both space and ground systems.

What a scanning radiometer views at any instant is called the Instantaneous Field Of View (IFOV) and it is generally considered as the spatial resolution of the imaging sensor. The size of an individual pixel or picture element also depends mainly on the sampling rate and the forward motion of the spacecraft. In a meteorological satellite, the spatial resolution of the radiometer will decide the smallest cloud that can be seen in the image.

The spectral resolution of the sensor is inversely related to the channel bandwidth. A higher spectral resolution and an accurate spectral signature can be obtained by having a large number of narrow bands, rather than one continuous broad band.

The term radiometric resolution is used to indicate the smallest perceptible change in the radiance of various targets that the sensor can discriminate. It is a measure of the signal-to-noise ratio of the sensor. It can also be defined in terms of the ability to resolve temperature difference between targets.

The temporal resolution is an important consideration in operational meteorology because it determines what kind of meteorological phenomena can be viewed by the satellite, as they have different lifetimes. Temporal resolution refers to the elapsed time interval between two successive satellite scans of a given region. This is also called the repeat cycle or repetivity of the orbit.

The temporal resolution is decided by the design of the scanning radiometer as well as the nature of the spacecraft orbit and it has to have a significant trade-off with the spatial resolution. For achieving a finer spatial resolution, the scan has to be made slower and the temporal resolution will get reduced. In a rapid scan, a selected area can be scanned repeatedly, but then other areas will be left out. Satellites meant for monitoring of earth resources or for cartographic applications can have an extremely high spatial and spectral resolution because they can afford to have a long repeat cycle.

1.4.2 Navigation and Gridding

In some VIS and IR satellite images, geographical features like coastlines, islands and lakes are distinctly seen, but many times they may be obscured because of clouding or a lack of temperature contrast. In WV images they are rarely noticeable. Therefore, for any satellite image to be used for practical purposes, it must be provided with a geographical reference frame. This last stage of the process of satellite image production actually involves three steps, navigation, gridding and registration.

The term navigation, also called geolocation, is used in its conventional sense as in flying, shipping or driving on a road. Image navigation makes it possible to relate every pixel, identified by its line and element number to a point on the earth, defined by its latitude and longitude, and vice versa.

By gridding is meant the superposition of names of locations, latitude-longitude lines or political boundaries on the navigated image. Once the mages are accurately geolocated, they can be transformed into desired cartographic projections like Mercator or Lambert and overlaid with maps.

If geostationary satellite images are viewed in quick succession, the surface features should appear to be stationary. The removal of apparent earth motion from an animated sequence of images is called registration.

The navigation and gridding process for a 3-axes stabilized geostationary satellite like INSAT has been explained in detail by Kelkar et al (1980). Briefly, it involves transformations among the following five coordinate systems:

(a) inertial system, having its origin at the centre of the dynamical earth, and the x-axis pointing to the vernal equinox and z-axis normal to the equatorial plane,

(b) rotating system, similar to the inertial system but with the z-axis passing through the Greenwich meridian,

(c) local vertical system, having its origin at the centre of the satellite,

(d) body-centred system, defined in terms of the pitch, roll and yaw angles, and

(e) picture frame system, defined in terms of line and element number.

In the actual process, Ground Control Points (GCPs) or precisely located earth features are used, and Global Positioning System (GPS) information for pinpointing the satellite location.

The accuracy of navigation has a very important bearing in quantitative product derivation like cloud motion winds or in lightning detection, in which the positions of the pixels have to be known very precisely. A poor navigation shows up as a mismatch between the superimposed grid and the geographical features on the image. Navigation errors may also result in image distortions. Channel-to-channel registration, frame-to-frame and within-frame registration are therefore all important (Tan et al 2020).

1.5 Indian Meteorological Satellites

The need for India to have its own meteorological and remote sensing satellite programme to monitor its weather and vast natural resources was realized way back in the 1960s by great pioneers and visionaries like Vikram Sarabhai and Satish Dhawan. The successful launches of the first Indian satellites Aryabhata, Bhaskara-I, Bhaskara-II and APPLE between 1975 and 1981 were followed by the launch of INSAT-1A in 1982 and INSAT-1B in 1983. The first Indian remote sensing satellite IRS-1A was launched in 1988. The evolution of the meteorological component of the Indian space programme has been reviewed from time to time by Kelkar (1994a, 1994b, 2009, 2019) and Bhatia (2025).

INSAT is India's unique multi-purpose geostationary satellite system which was conceptualized to bring in satellite-based services in as many fields

as possible in the shortest time. In contrast with other countries that had dedicated satellites for different purposes, INSAT ushered in a new era in communications, television and radio broadcasting, and meteorology with a single satellite. Since 1965, Indian weather forecasters were having a limited access to low resolution satellite imagery of foreign satellites through the APT facility. It was only with the launch of the INSAT-1A satellite in 1982 that satellite meteorology may be said to have truly come of age in India.

Table 1.5 gives the chronology of the evolution of the INSAT meteorological programme. While the INSAT-1 series consisted of multi-purpose satellites, some of the later satellites did not have any meteorological component. On the other hand, Metsat, launched in 2002 was exclusively dedicated to meteorological imaging. Likewise, INSAT-3D, -3DR and -3DS, launched in recent years, are primarily meteorological satellites without any communication transponders except for data relay and satellite-aided search and rescue. INSAT-2E was the first geostationary meteorological satellite to have a CCD payload. INSAT-3D was the first Indian satellite with a sounder.

Satellites in the INSAT-1 series were designed by ISRO but built in the U.S. and launched from abroad. Satellites in the INSAT-2 series were built indigenously but launched from abroad. Metsat, was launched from Sriharikota by ISRO's Polar Satellite Launch Vehicle (PSLV). It was later renamed Kalpana-1 in memory of Dr Kalpana Chawla, the India-born American astronaut who perished in the U.S. Space Shuttle Columbia disaster on 1 February 2003. Satellites in the INSAT-3 series have been built by ISRO and launched with its own Geostationary Launch Vehicle (GSLV).

Table 1.5.1 Chronology of the Evolution of the INSAT Meteorological Programme.

Name of Satellite	Launch Date	Meteor-logical Payload	Channel	Spectral Range (μ)	Resolu-tion (km)
INSAT-1A	10 April 1982	VHRR (Very High Resolution Radiometer)	VIS IR	0.55-0.75 10.5-12.5	2.75 11
INSAT-1B	30 August 1983	VHRR			
INSAT-1C	21 July 1988	VHRR			
INSAT-1D	12 June 1990	VHRR			

Table 1.5.1 *Contd….*

Name of Satellite	Launch Date	Meteor-logical Payload	Channel	Spectral Range (μ)	Resolu-tion (km)
INSAT-2A	10 July 1992	VHRR	VIS IR	0.55-0.75 10.5-12.5	2 8
INSAT-2B	23 July 1993	VHRR			
INSAT-2E	3 April 1999	VHRR	VIS IR WV	0.55-0.75 10.5-12.5 5.7-7.1	2 8 8
		CCD Charge Coupled Device Camera	VIS NIR SWIR	0.62-0.68 0.77-0.86 1.55-1.69	1 1 1
Metsat/ Kalpana-1	12 September 2002	VHRR	VIS IR WV	0.55-0.75 10.5-12.5 5.7-7.1	2 8 8
INSAT-3A	10 April 2003	VHRR	VIS IR WV	0.55-0.75 10.5-12.5 5.7-7.1	2 8 8
		CCD	VIS NIR SWIR	0.62-0.68 0.77-0.86 1.55-1.69	1 1 1
INSAT-3D	26 July 2013	VHRR	VIS SWIR MWIR WV TIR TIR	0.55-0.75 1.55-1.70 3.80-4.00 6.50-7.10 10.3-11.3 11.5-12.5	1 1 4 8 4 4
NSAT-3DR	6 September 2015				
INSAT-3DS	13 February 2024	Sounder	SWIR MWIR LWIR VIS	3.67-4.59 6 channels 6.38-11.33 5 channels 11.66-14.85 7 channels 0.67-0.72 1 channel	10 10 10 10

1.6 References

Bhatia, R. C. and Gupta, H. V., 1999, "Use of charged coupled device payload on INSAT-2E for meteorological and agricultural applications", *Current. Sci.*, 1999, 76, 1444–1447.

Bhatia R. C. and Mitra A. K.. 2025, "Evolution of satellite meteorology and its future scope - India's perspective" *Mausam*, 76, 31-54.

Datar S. V. and Joseph C. P., 1971, "A satellite automatic picture transmission (APT) system ground receiving station", *Indian J. Meteor. Geophys.*, 22, 377-380.

Gohil B. S. and co-authors, 1982, "Remote sensing of atmospheric water content from Bhaskara SAMIR data", *Int. J. Remote Sensing*, 3, 235-241.

Hinsman D. E., 2006, "WMO Space Programme implementation activities", *14th Conf. Satellite Meteorology Oceanography*, Amer. Meteor. Soc.

Iyengar V. S. et al, 1999, "Meteorological imaging instruments on-board INSAT-2E", *Current Sci.,* 76, 1436-1443.

Kelkar R. R., Sant Prasad and Ellickson J., 1980, "Image navigation and gridding for three-axis stabilized geostationary satellites", *NOAA/NESDIS Report*, Washington DC, 32 pp.

Kelkar R. R., Sant Prasad and Khanna P. N., 1982, "Conception of an equatorial orbiting meteorological satellite for the tropics", *Mausam*, 33, 507-508.

Kelkar R. R., 1994a, "Satellites for monitoring climate change: the emerging scenario", *Proc. Indian National Science Academy*, 60, 335-348.

Kelkar R. R., 1994b, "Satellite meteorology in India – an overview", *Indian J. Radio Space Phys.*, 23, 235-245.

Kelkar R. R., 2009, "Evolution of satellite meteorology and its future scope", *Mausam, Diamond Jubilee Volume, Special Issue.*

Kelkar R. R., 2019, "Satellite meteorology in India: its beginning, growth and future", *Mausam*, 70, 1-14.

Mohapatra M. et al, 2021, "INSAT-3DR-rapid scan operations for weather monitoring over India", *Current Sci.*, 120, 1026-1034.

Padmanabhan N., Ramakrishnan R. and Gurjar S. B., 2004, "Geometric modelling of INSAT-2E CCD payload and multistrip mosaicing for geocoding large areas", *Current Sci*., 86, 1113-1121.

Pandey P. C., 1995, "Satellite-borne microwave radiometry for atmospheric studies", *Indian J. Radio Space Phys*., 24, 245-254.

Pathak P. N. and Gautam N., 1992, "Latitudinal distribution of water vapour over the Arabian Sea and Bay of Bengal using Bhaskara-II SAMIR data", *Mausam*, 43, 385-394.

Smith W. L. et al, 2002, "GIFTS-the precursor geostationary satellite component of the future Earth Observing System*",. Geoscience and Remote Sensing Symp. IGARSS'02*, 357-361.

Tan B. et al, 2020, "GOES-R series image navigation and registration performance assessment tool set", *J. Applied Remote Sensing*, 14, 032405-032405.

Trishchenko A. P., Garand L., and Trichtchenko L. D., 2019, "Observing polar regions from space: comparison between highly elliptical orbit and medium earth orbit constellations", *J. Atmos. Oceanic Techno.*, 36, 1605-1621.